# Identification of a uranium–rhodium triple bond in a heterometallic cluster

Genfeng Feng[a], Mingxing Zhang[a], Penglong Wang[a], Shuao Wang[b], Laurent Maron[c,1], and Congqing Zhu[a,1]

[a]State Key Laboratory of Coordination Chemistry, Jiangsu Key Laboratory of Advanced Organic Materials, School of Chemistry and Chemical Engineering, Nanjing University, 210023 Nanjing, China; [b]State Key Laboratory of Radiation Medicine and Protection, School for Radiological and interdisciplinary Sciences (RAD-X) and Collaborative Innovation Center of Radiation Medicine of Jiangsu Higher Education Institutions, Soochow University, 215123 Suzhou, China; and [c]Laboratoire de Physique et Chimie des Nanoobjets (LPCNO), Institut National des Sciences Appliquées (INSA) de Toulouse, 31077 Toulouse, France

Edited by Christopher C. Cummins, Massachusetts Institute of Technology, Cambridge, MA, and approved August 1, 2019 (received for review March 21, 2019)

**The chemistry of *d*-block metal–metal multiple bonds has been extensively investigated in the past 5 decades. However, the synthesis and characterization of species with *f*-block metal–metal multiple bonds are significantly more challenging and such species remain extremely rare. Here, we report the identification of a uranium–rhodium triple bond in a heterometallic cluster, which was synthesized under routine conditions. The uranium–rhodium triple-bond length of 2.31 Å in this cluster is only 3% longer than the sum of the covalent triple-bond radii of uranium and rhodium (2.24 Å). Computational studies reveal that the nature of this uranium–rhodium triple bond is 1 covalent bond with 2 rhodium-to-uranium dative bonds. This heterometallic cluster represents a species with *f*-block metal–metal triple bond structurally authenticated by X-ray diffraction. These studies not only demonstrate the authenticity of the uranium–metal triple bond, but also provide a possibility for the synthesis of other *f*-block metal–metal multiple bonds. We expect that this work may further our understanding of the bonding between uranium and transition metals, which may help to design new *d-f* heterometallic catalysts with uranium–metal bonds for small-molecule activation and to promote the utilization of abundant depleted uranium resources.**

chemical bonding | metal–metal bond | uranium–metal multiple bond | heterometallic cluster | DFT

Molecules with metal–metal bonds have long interested both theoreticians and experimental scientists because of their fascinating structures (1–4). In a seminal study, Cotton et al. (1) proposed a rhenium–rhenium quadruple bond in $[Re_2Cl_8]^{2-}$ species. Since then, the chemistry of *d*-block transition metal–metal multiple bonds has flourished (5–7).

However, for the *f*-block lanthanide and actinide metals, the situation is more complicated if the *f*-orbital electrons are involved in metal–metal bonding (8). For instance, although the first species with a uranium–metal single bond was reported in 1987 (9), published examples of structures containing a uranium–metal bond have only begun to grow slowly in the past decade (10–14). Therefore, it is understandable that the study of *f*-block metal–metal multiple bonds remains scarce, perhaps due to the extreme difficulty of their synthesis and structural characterization. More recent works have tried to explore the chemistry of actinide–metal multiple bonds through theoretical calculations (15–24). Gagliardi and Roos (16), for example, theoretically predicted the quintuple-bond character in the uranium molecule $U_2$ in 2005. Interestingly, such a molecule was reported recently by Knecht et al. and shown by state-of-the-art relativistic quantum-chemical calculations to contain a quadruple bond (24). Two recent landmark experimental advances in this field are the generation of a U–Fe triple bond in the gas phase under laser vaporization by Zhou and coworkers (25) and the synthesis of a double-dative bond between Rh and U by Liddle and coworkers (26).

Despite such remarkable progress in this area, no examples of species with *f*-block metal–metal triple bonds structurally authenticated by X-ray crystallography have been reported. Here, we report an unprecedented heterometallic cluster containing 2 uranium–rhodium triple bonds. This molecule represents an authentic example of *f*-block metal–metal triple bond, which can be synthesized under routine conditions and characterized by X-ray diffraction and quantum-chemical calculations.

## Results and Discussion

Recently, we demonstrated the synthesis of heterometallic complexes with multiple uranium–nickel bonds by the reaction of complex **1** with zero-valent transition-metal complex, $Ni(COD)_2$ (COD = cyclo-octadiene) (27). With complex **1** in hand, we thus investigated the reaction between **1** and monovalent transition-metal species. As shown in Fig. 1, following treatment of complex **1** with 1 equivalent of $[RhCl(COD)]_2$ at room temperature (RT) in tetrahydrofuran, complex **2** was isolated as brown crystals in 58% yield after 24 h. Use of additional $[RhCl(COD)]_2$ did not alter the product. A mixture of crystalline **2** with 6 equivalents of potassium–graphite ($KC_8$) in tetrahydrofuran over 12 h at RT led to the crystalline complex **3** in 26% yield as black crystals after straightforward workup. Both **2** and **3** are stable in the absence of air and moisture and were characterized by elemental analysis, infrared spectroscopy, and X-ray powder diffraction in their solid state (*SI Appendix*, Figs. S1–S4). The colors of **2** and **3** can be explained by the strong absorption in the UV-visible region of their electronic absorption spectra. Complex **2** displays absorption

### Significance

**Multimetallic species exhibit great potential in catalysis and small-molecule activation due to their multimetallic synergistic effects. Biological nitrogen fixation and industrial Haber–Bosch processes for ammonia synthesis are thought to involve multimetallic catalytic sites. Uranium-based materials were used as effective catalysts for ammonia production from nitrogen before an iron-based catalyst was used for the current industrial Haber–Bosch process. However, the synthesis and characterization of multimetallic species with uranium–metal bonds are significantly more challenging and no complex with *f*-block metal–metal triple bonds have been structurally authenticated by X-ray crystallography thus far. Here we report the identification of a *d-f* heterometallic cluster with 2 uranium–rhodium triple bonds.**

Author contributions: L.M. and C.Z. designed research; G.F., M.Z., and P.W. performed research; S.W. contributed new reagents/analytic tools; and L.M. and C.Z. wrote the paper.

The authors declare no conflict of interest.

This article is a PNAS Direct Submission.



[1]To whom correspondence may be addressed. Email: laurent.maron@irsamc.ups-tlse.fr or zcq@nju.edu.cn.

This article contains supporting information online at www.pnas.org/lookup/suppl/doi:10.1073/pnas.1904895116/-/DCSupplemental.

Published online August 19, 2019.

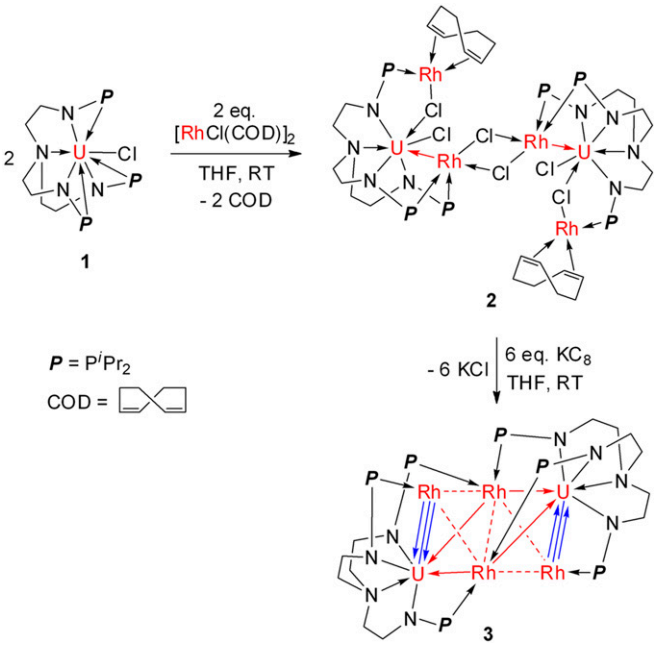


**Fig. 1.** Synthesis of heterometallic clusters **2** and **3**. Complex **2** was isolated from the reaction between **1** and $[RhCl(COD)]_2$ and cluster **3** was prepared from complex **2** by treatment of it with 6 equivalents of $KC_8$. THF = tetrahydrofuran, $KC_8$ = potassium–graphite.

from 300 to 500 nm with a band centered at 400 nm (molar absorption coefficient, ε = ~2,522 $M^{-1}{\cdot}cm^{-1}$), whereas complex **3** exhibits broad absorption from 300 to 900 nm, with a band centered at 494 nm (ε = ~5,307 $M^{-1}{\cdot}cm^{-1}$) and extending to the near-infrared region (*SI Appendix*, Fig. S5).

The molecular structure of complex **2** was determined by X-ray diffraction crystallography, which showed it to be a centrosymmetric dimer (Fig. 2). The length of the U1–Rh2 bond is 2.9609(7) Å, which is very close to the sum of the covalent single-bond radii for uranium and rhodium (2.95 Å) (28). The formal shortness ratio (FSR) defined as the ratio of the metal–metal bond length to the sum of the covalent atomic radii of the 2 metals (29), has been widely used to evaluate the bonding between 2 metals (30). The value of FSR for U1–Rh2 in complex **2** is 1.00. This complex is an unusual example of a dichloro-bridged multimetallic cluster with *f*-block metal–metal bonds.

An X-ray diffraction study performed upon a single crystal of complex **3** obtained from a toluene solution at −30 °C revealed that the 4 rhodium atoms form a diamond-shaped quadrilateral with Rh2 and Rh4 as bridged atoms connecting U1 and U2, leading to the formation of 2 pyramids formed by 6 U–Rh bonds (Fig. 3). This is the highest number of U–Rh bonds observed in a molecule. The bond lengths of U1–Rh2 [2.9740(10) Å], U1–Rh4 [2.8976(10) Å], U2–Rh2 [2.9445(12) Å], and U2–Rh4 [2.9788 (11) Å] are close to the U–Rh bond distance [2.9609(7) Å] observed in **2**. All of the FSR values for these U–Rh bonds are close to 1.00, suggesting the dative bonds of these U–Rh interactions. The Rh···Rh distances [range from 2.8027(14) Å to 3.0317 (15) Å] in complex **3** are obviously longer than the sum of single-bond covalent radii for 2 rhodium atoms (2.50 Å), which indicate the weak Rh–Rh interactions between these rhodium atoms. The calculated Rh–Rh Wiberg bond orders are in the range of 0.18 to 0.44, consistent with weak Rh–Rh bonding characters.

The most salient feature of **3** is that the bond lengths of U1–Rh1 [2.3164(9) Å] and U2–Rh3 [2.3125(10) Å] are significantly shorter than the other U–Rh bonds in this cluster. Both of these 2 U–Rh bonds are also significantly shorter than the U–Rh double-dative bond [2.5835(3) Å] reported previously (26). The U1–Rh1 and U2–Rh3 bond lengths are even shorter than the sum of the covalent double-bond radii of uranium and rhodium (2.44 Å) and only 0.07 Å (3%) longer than the sum of the covalent triple-bond radii of uranium and rhodium (2.24 Å) (31, 32). The U1–Rh1 and U2–Rh3 bond lengths are the shortest example observed to date for any *f*-element transition-metal bond measured by X-ray crystallography. The FSR values for U1-Rh1 and U2-Rh3 are 0.785 [compare $FSR(N_2) = 0.786$], which are close to the FSRs for the transition-metal–metal triple bond (33), indicating 2 U–Rh triple bonds in complex **3**. The U1–Rh1 and U2–Rh3 bond distances in complex **3** are close to the U–Ir triple-bond lengths in NUIr (2.21 Å) and $OUIr^+$ (2.18 Å), which are predicted by Gagliardi and Pyykkö (15) and synthesized by Santos et al. in the gas phase employed laser desorption/ionization method (34). In addition, analogous species containing Th–Ir triple bond was also predicted theoretically (35), which suggests that the species with Th–M triple bond could be synthesized under normal experimental conditions. Nevertheless, complex **3** represents a species with *f*-block metal–metal triple bond structurally authenticated by X-ray diffraction.

The variable-temperature magnetic data for both **2** and **3** were measured with a superconducting quantum interference device (SQUID) in the solid state. The magnetic moment of **2** at 300 K is 5.06 $\mu_B$ (3.58 $\mu_B$ per uranium ion), which gradually decreases to 0.77 $\mu_B$ (0.54 $\mu_B$ per uranium ion) at low temperature (5 K) and toward zero (Fig. 4). These magnetic data and the temperature dependency are consistent with typical uranium(IV) centers with a $5f^2$ configuration. The trend of the magnetic moment for **3** is similar to that of complex **2**, which also shows a strong temperature dependency (Fig. 4). The magnetic data of **3** at 5 K (0.90 $\mu_B$) and 300 K (6.06 $\mu_B$) are slightly higher than those observed for **2**. The higher magnetic moment for **3** is probably a result of the strongly donating groups on the uranium(IV) center

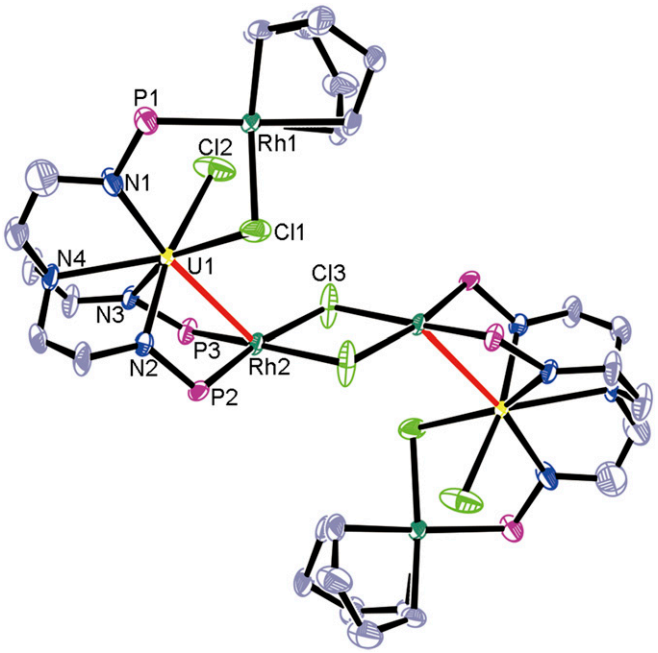


**Fig. 2.** Molecular structure of **2** (with 50% probability ellipsoids). Solvent molecules, hydrogen atoms, and isopropyl moieties in $P^iPr_2$ are omitted for clarity. Selected bond distances (Å): U1–Rh2 2.9609(7), U1–Cl1 2.780(2), U1–Cl2 2.686(3), Rh1–Cl1 2.431(3), Rh2–Cl3 2.391(2). Estimated SDs are in parentheses. Uranium, yellow; rhodium, green; phosphorus, violet red; nitrogen, blue; chlorine, yellow–green; carbon, gray.

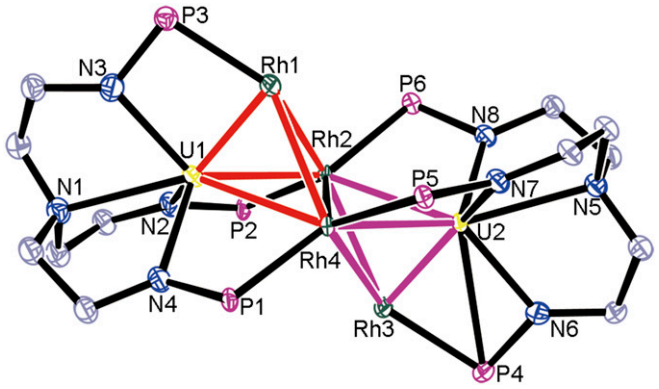


**Fig. 3.** Molecular structure of **3** (with 50% probability ellipsoids). Solvent molecules, hydrogen atoms, and isopropyl moieties in $P^iPr_2$ are omitted for clarity. Selected bond distances (Å): U1–Rh1 2.3164(9), U1–Rh2 2.9740(10), U1–Rh4 2.8976(10), U2–Rh2 2.9445(12), U2–Rh3 2.3125(10), U2–Rh4 2.9788(11), Rh1–Rh2 2.8815(14), Rh2–Rh3 3.0317(15), Rh3–Rh4 2.8027(14), Rh4–Rh1 2.8858(14), Rh2–Rh4 2.9511(16). Estimated SDs are in parentheses. Uranium, yellow; rhodium, green; phosphorus, violet red; nitrogen, blue; carbon, gray.

(26, 36–39), and is consistent with the short uranium–rhodium triple bond. The similar magnetic behaviors of **2** and **3** are however in agreement with the assignment of a uranium(IV) oxidation state.

X-ray photoelectron spectroscopy measurements were carried out to investigate the oxidation states of rhodium and uranium in both **2** and **3** (*SI Appendix*, Figs. S6 and S7). The uranium $4f_{7/2}$ binding energies of **2** and **3** were observed to be 381.7 and 381.5 eV, respectively. Therefore, the oxidation states of uranium ions in both **2** and **3** are identical (+4), which is consistent with the result of SQUID analysis. The formal oxidation states of the 2 triply bonded rhodium centers (Rh1 and Rh3) in complex **3** can be assigned as Rh(-I), whereas the other 2 rhodium centers (Rh2 and Rh4) are in zero oxidation state. These assignments are consistent with the fact that complex **3** was synthesized by a 6-electron reduction of complex **2**.

Density functional theory (DFT) calculations were performed to elucidate the nature of the bonding in **3**. The computational strategy employed is similar to that used in an earlier study of $U_2Ni_n$ complexes (27). Geometry optimization using small-core Relativistic Effective Core Potential (RECP), which explicitly treats the 5*f* electrons on uranium, was carried out on complex **3**. The optimized geometry was found to be in excellent agreement with the experimental data. The U–Rh distances were computed to be 2.31 Å (U1–Rh1 and U2–Rh3) and 2.89 Å (U1–Rh2, U1–Rh4 and U2–Rh2, U2–Rh4), consistent with the experimentally determined structure. The Natural Population Analysis is in line with the formal oxidation states of the rhodium centers (Rh1,Rh3: −0.8 with a formal oxidation state of –I and Rh2,Rh4 = −0.06 in line with a zero oxidation state). The lowest spin state is a quintet, describing 2 unpaired spins on each U and U(IV) center. Complete active-space self-consistent field calculations were carried out in order to determine the nature of the first low-lying excited states. Distributing 6 electrons into 6 orbitals (2 5f orbitals on each uranium center and a 5d orbital on Rh2 and Rh4) yields to a quintet ground state, that is a ferromagnetic coupling between the 2 U and an antiferromagnetic coupling between the 2 Rh. An open-shell singlet was found to be the first excited state at +0.38 eV, that consists of an antiferromagnetic coupling between the 2 U and an antiferromagnetic coupling between the 2 Rh. The septet state, that would involve a ferromagnetic coupling between the 2 U and a ferromagnetic coupling between the 2 Rh, is lying very high in energy (+3.56 eV). The nature of the uranium oxidation state as well as of the Rh2–Rh4 magnetic coupling was further confirmed by optimizing the structure using an *f*-in-core RECP adapted to the U(IV) oxidation state. Indeed, both a singlet (antiferromagnetic coupling) and triplet (ferromagnetic coupling) were optimized. The singlet was found to be lower in energy and the associated overall structure is well-reproduced even though the U1–Rh1 and U2–Rh3 bond lengths are longer than the experimental ones (2.34 Å versus the experimental 2.31 Å). Scrutinizing the molecular orbitals of complex **3**, 1 σ and 2 π bonding U1–Rh1/U2–Rh3 orbitals are found but they all involve the 4 Rh atoms and the 2 U atoms making the picture somewhat unclear (*SI Appendix*, Fig. S10). Consequently, a natural bond orbital (NBO) analysis was carried out. The Wiberg indexes (WBIs) are in line with a triple-bond U1–Rh1/U2–Rh3 (WBIs of 2.61) and single bonds U1,2–Rh2,4 (WBIs of 0.85). For sake of comparison, the Rh–Rh WBIs are in between 0.18 and 0.44, indicating some Rh–Rh interaction. For the U1–Rh1 and U2–Rh3 interactions, a σ U–Rh bond is found at the first-order NBO that involves an *s*/*d*/*f* hybrid orbital (20, 38, and 42%) on uranium and a *d* orbital on Rh. At the second order, 2 strong donations (95 and 88 kcal $mol^{-1}$) from filled *d* orbitals of Rh into empty *d*/*f* hybrid (24 and 76%) orbitals of U are found. Therefore, all analyses point to the presence of 2 U–Rh triple bonds in the heterometallic cluster **3** (Fig. 5). For sake of comparison, geometry optimization and NBO analysis were also carried out on complex **2**. The optimized geometry is in agreement with the experimental one. For instance, the U–Rh bond is computed to be 3.01 Å (vs. 2.96 Å experimentally) and the U–Cl ones to be 2.73 and 2.81 (vs. 2.69 and 2.78 Å experimentally). At the NBO level, a σ U–Rh bond is found formed with an *s*/*d*/*f* hybrid orbital (17, 39, and 44%) on uranium and a *d* orbital on Rh. At the second order no substantial donation from Rh to U is found, indicating that no more bonding interaction between U and Rh is present. The WBI of U1-Rh2 in complex **2** was also computed and it is found to be 0.88, in line with a single-bond character. This value is similar to what was found in complex **3** between $U_{1,2}$ and $Rh_{2,4}$ and very different from the results found for the U1–Rh1 and U2–Rh3 bonds.

Multimetallic complexes have attracted interest in catalysis and small-molecule activation owing to their multimetallic

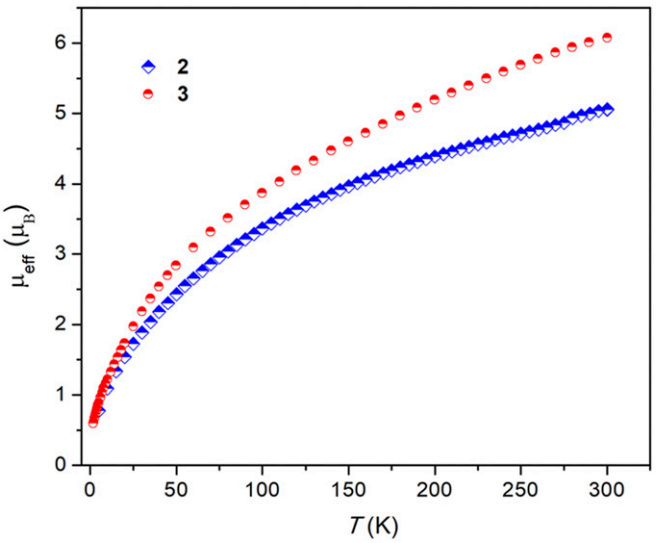


**Fig. 4.** Variable-temperature magnetism studies of heterometallic clusters **2** and **3** by SQUID magnetometry. The magnetic behaviors exhibit strong temperature dependency trending to zero at low temperature, indicating uranium(IV) centers in both **2** and **3**.

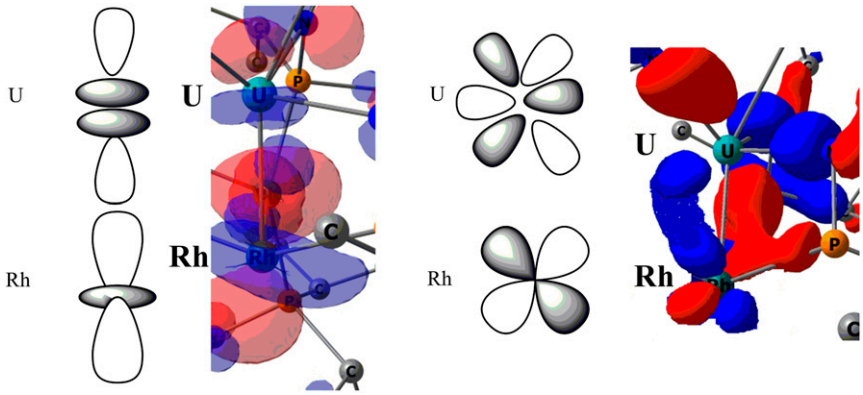


**Fig. 5.** Two-dimensional and three-dimensional representation of the molecular orbitals describing the σ (*Left*) and one of the π (*Right*) U–Rh interactions. A zoom of the bonding part is only reported here whereas the full picture in given in *SI Appendix*, Fig. S10.

synergistic effects. Cooperativity of multiple metal centers can facilitate multielectron redox which is difficult for monometallic species. The $N_2$ reduction and industrial Haber–Bosch processes for ammonia synthesis are thought to involve multimetallic catalytic sites. Uranium species exhibits promising properties in small-molecule activation (40–46). The dative U ← Rh bonds in the *d-f* heterometallic clusters **2** and **3** are advantageous for synergistic substrate activation through the polarized U–Rh bond. In addition, both **2** and **3** exhibit strong absorption in the UV-visible region, which enables their potential application in metallaphotocatalysis (47).

## Conclusions

In summary, we report a uranium–rhodium triple bond in a heterometallic molecular cluster. A study of this cluster indicates that the compound containing 2 uranium–metal triple bonds can be prepared, isolated, and characterized under routine conditions. Thus, this species represents an example of *f*-block metal–metal triple bond whose structure has been authenticated by X-ray diffraction. The corresponding FSR value of this triple bond is only 0.785, and is comparable to the FSR values for the transition-metal–metal triple bond. DFT calculations reveal that the nature of this triple bond is 1 covalent σ bond with 2 rhodium-to-uranium dative bonds. This molecule can be used as a model for studying the uranium–metal triple bond. This study not only provides a synthetic strategy for the construction of *d-f* heterometallic clusters with metal–metal multiple bonds but also may promote the utilization of abundant depleted uranium resources in small-molecule activation and metallaphotocatalysis.

## Materials and Methods

All reactions were carried out using a Vigor Ar-atmosphere glove box (<1 ppm $O_2/H_2O$). Solvents were dried and degassed before use through a Mikrouna solvent drying system. Samples were carefully checked for purity and reproducibility of their data. Details concerning the synthesis and characterization of other complexes can be found in *SI Appendix*. Single-crystal X-ray diffraction data for complexes **2** and **3** were collected at 123 K on a Bruker D8 complementary metal oxide semiconductor detector using graphite-monochromated Mo Kα radiation (λ = 0.71073 Å). X-ray crystal structures have been deposited in the Cambridge Crystallographic Database under the deposition numbers CCDC 1886167 (**2**) and 1886168 (**3**). These data can be obtained free of charge via https://www.ccdc.cam.ac.uk/structures/. Details of single-crystal X-ray diffraction experiments and computational studies can be found in *SI Appendix*.

**ACKNOWLEDGMENTS.** We thank Dr. Yue Zhao at Nanjing University for assistance with X-ray crystallography. This research was supported by the National Natural Science Foundation of China (Grant 21772088), the Natural Science Foundation of Jiangsu Province (Grant BK20170635), the Young Elite Scientist Sponsorship Program of China Association of Science and Technology, the program of Jiangsu Specially-Appointed Professor, and Shuangchuang Talent Plan of Jiangsu Province.

1. F. A. Cotton *et al.*, Mononuclear and polynuclear chemistry of rhenium (III): Its pronounced homophilicity. *Science* **145**, 1305–1307 (1964).
2. I. Resa, E. Carmona, E. Gutierrez-Puebla, A. Monge, Decamethyldizincocene, a stable compound of Zn(I) with a Zn-Zn bond. *Science* **305**, 1136–1138 (2004).
3. M. S. Hill, P. B. Hitchcock, R. Pongtavornpinyo, A linear homocatenated compound containing six indium centers. *Science* **311**, 1904–1907 (2006).
4. S. P. Green, C. Jones, A. Stasch, Stable magnesium(I) compounds with Mg-Mg bonds. *Science* **318**, 1754–1757 (2007).
5. E. P. Kundig, M. Moskovits, G. A. Ozin, Matrix synthesis and characterization of dichromium. *Nature* **254**, 503–504 (1975).
6. T. Nguyen *et al.*, Synthesis of a stable compound with fivefold bonding between two chromium(I) centers. *Science* **310**, 844–847 (2005).
7. F. R. Wagner, A. Noor, R. Kempe, Ultrashort metal-metal distances and extreme bond orders. *Nat. Chem.* **1**, 529–536 (2009).
8. M. V. Butovskii *et al.*, Molecules containing rare-earth atoms solely bonded by transition metals. *Nat. Chem.* **2**, 741–744 (2010).
9. R. S. Sternal, T. J. Marks, Actinide-to-transition metal bonds. Synthesis, characterization, and properties of metal-metal bonded systems having the tris(cyclopentadienyl) actinide fragment. *Organometallics* **6**, 2621–2623 (1987).
10. B. M. Gardner, J. McMaster, W. Lewis, S. T. Liddle, Synthesis and structure of $[\{N(CH_2CH_2NSiMe_3)_3\}URe(\eta^5\text{-}C_5H_5)_2]$: A heterobimetallic complex with an unsupported uranium-rhenium bond. *Chem. Commun. (Camb.)*, 2851–2853 (2009).
11. B. M. Gardner *et al.*, An unsupported uranium-rhenium complex prepared by alkane elimination. *Chem. Eur. J.* **17**, 6909–6912 (2011).
12. J. W. Napoline *et al.*, Tris(phosphinoamide)-supported uranium-cobalt heterobimetallic complexes featuring Co → U dative interactions. *Inorg. Chem.* **52**, 12170–12177 (2013).
13. A. L. Ward, W. W. Lukens, C. C. Lu, J. Arnold, Photochemical route to actinide-transition metal bonds: Synthesis, characterization and reactivity of a series of thorium and uranium heterobimetallic complexes. *J. Am. Chem. Soc.* **136**, 3647–3654 (2014).
14. J. A. Hlina, J. R. Pankhurst, N. Kaltsoyannis, P. L. Arnold, Metal-metal bonding in uranium-group 10 complexes. *J. Am. Chem. Soc.* **138**, 3333–3345 (2016).
15. L. Gagliardi, P. Pyykkö, Theoretical search for very short metal-actinide bonds: NUIr and isoelectronic systems. *Angew. Chem. Int. Ed. Engl.* **43**, 1573–1576 (2004).
16. L. Gagliardi, B. O. Roos, Quantum chemical calculations show that the uranium molecule $U_2$ has a quintuple bond. *Nature* **433**, 848–851 (2005).
17. L. Gagliardi, P. Pyykkö, B. O. Roos, A very short uranium-uranium bond: The predicted metastable $U_2^{2+}$. *Phys. Chem. Chem. Phys.* **7**, 2415–2417 (2005).
18. M. Straka, P. Pyykkö, Linear HThThH: A candidate for a Th-Th triple bond. *J. Am. Chem. Soc.* **127**, 13090–13091 (2005).
19. B. O. Roos, L. Gagliardi, Quantum chemistry predicts multiply bonded diuranium compounds to be stable. *Inorg. Chem.* **45**, 803–807 (2006).
20. G. La Macchia, M. Brynda, L. Gagliardi, Quantum chemical calculations predict the diphenyl diuranium compound [PhUUPh] to have a stable $^1A_g$ ground state. *Angew. Chem. Int. Ed. Engl.* **45**, 6210–6213 (2006).
21. B. O. Roos, P. Å. Malmqvist, L. Gagliardi, Exploring the actinide-actinide bond: Theoretical studies of the chemical bond in $Ac_2$, $Th_2$, $Pa_2$, and $U_2$. *J. Am. Chem. Soc.* **128**, 17000–17006 (2006).
22. C. Z. Wang *et al.*, Actinide (An = Th-Pu) dimetallocenes: Promising candidates for metal-metal multiple bonds. *Dalton Trans.* **44**, 17045–17053 (2015).
23. H. S. Hu, N. Kaltsoyannis, The shortest Th-Th distance from a new type of quadruple bond. *Phys. Chem. Chem. Phys.* **19**, 5070–5076 (2017).

24. S. Knecht, H. J. A. Jensen, T. Saue, Relativistic quantum chemical calculations show that the uranium molecule $U_2$ has a quadruple bond. *Nat. Chem.* **11**, 40–44 (2019).
25. C. Chi *et al*., Preparation and characterization of uranium-iron triple-bonded UFe(-CO)$^{3-}$ and OUFe(CO)$^{3-}$ complexes. *Angew. Chem. Int. Ed. Engl.* **56**, 6932–6936 (2017).
26. E. Lu, A. J. Wooles, M. Gregson, P. J. Cobb, S. T. Liddle, A very short uranium(IV)-rhodium(I) bond with net double-dative bonding character. *Angew. Chem. Int. Ed. Engl.* **57**, 6587–6591 (2018).
27. G. Feng *et al*., Transition-metal-bridged bimetallic clusters with multiple uranium-metal bonds. *Nat. Chem.* **11**, 248–253 (2019).
28. P. Pyykkö, M. Atsumi, Molecular single-bond covalent radii for elements 1-118. *Chem. Eur. J.* **15**, 186–197 (2009).
29. F. A. Cotton, C. A. Murillo, R. A. Walton, *Multiple Bonds Between Metal Atoms* (Springer Science & Business Media, Inc., New York, ed. 3, 2005).
30. R. H. Duncan Lyngdoh, H. F. Schaefer, 3rd, R. B. King, Metal-metal (MM) bond distances and bond orders in binuclear metal complexes of the first row transition metals titanium through zinc. *Chem. Rev.* **118**, 11626–11706 (2018).
31. P. Pyykkö, Additive covalent radii for single-, double-, and triple-bonded molecules and tetrahedrally bonded crystals: A summary. *J. Phys. Chem. A* **119**, 2326–2337 (2015).
32. P. Pyykkö, S. Riedel, M. Patzschke, Triple-bond covalent radii. *Chem. Eur. J.* **11**, 3511–3520 (2005).
33. F. A. Cotton, J. H. Matonic, C. A. Murillo, A new type of divalent niobium compound: The first Nb-Nb triple bond in a tetragonal lantern environment. *J. Am. Chem. Soc.* **119**, 7889–7890 (1997).
34. M. Santos, J. Marcalo, A. Pires de Matos, J. K. Gibson, R. G. Haire, Actinide-transition metal heteronuclear ions and their oxides: $\{IrUO\}^+$ as an analogue to uranyl. *Eur. J. Inorg. Chem.*, 3346–3349 (2006).
35. P. Hrobárik, M. Straka, P. Pyykkö, Computational study of bonding trends in the metalloactinyl series EThM and MThM′ (E = $N^-$, O, $F^+$; M, M′ = $Ir^-$, Pt, $Au^+$). *Chem. Phys. Lett.* **431**, 6–12 (2006).
36. J. L. Brown, S. Fortier, R. A. Lewis, G. Wu, T. W. Hayton, A complete family of terminal uranium chalcogenides, $[U(E)(N\{SiMe_3\}_2)_3]^-$ (E = O, S, Se, Te). *J. Am. Chem. Soc.* **134**, 15468–15475 (2012).
37. D. P. Halter, H. S. La Pierre, F. W. Heinemann, K. Meyer, Uranium(IV) halide ($F^-$, $Cl^-$, $Br^-$, and $I^-$) monoarene complexes. *Inorg. Chem.* **53**, 8418–8424 (2014).
38. B. M. Gardner *et al*., Triamidoamine uranium(IV)-arsenic complexes containing one-, two- and threefold U-As bonding interactions. *Nat. Chem.* **7**, 582–590 (2015).
39. M. Gregson *et al*., The inverse-trans-influence in tetravalent lanthanide and actinide bis(carbene) complexes. *Nat. Commun.* **8**, 14137 (2017).
40. A. R. Fox, S. C. Bart, K. Meyer, C. C. Cummins, Towards uranium catalysts. *Nature* **455**, 341–349 (2008).
41. B. M. Gardner *et al*., Homologation and functionalization of carbon monoxide by a recyclable uranium complex. *Proc. Natl. Acad. Sci. U.S.A.* **109**, 9265–9270 (2012).
42. D. P. Halter, F. W. Heinemann, J. Bachmann, K. Meyer, Uranium-mediated electrocatalytic dihydrogen production from water. *Nature* **530**, 317–321 (2016).
43. M. Falcone, L. Chatelain, R. Scopelliti, I. Živković, M. Mazzanti, Nitrogen reduction and functionalization by a multimetallic uranium nitride complex. *Nature* **547**, 332–335 (2017).
44. P. L. Arnold, Z. R. Turner, Carbon oxygenate transformations by actinide compounds and catalysts. *Nat. Rev. Chem.* **1**, 0002 (2017).
45. D. P. Halter, F. W. Heinemann, L. Maron, K. Meyer, The role of uranium-arene bonding in $H_2O$ reduction catalysis. *Nat. Chem.* **10**, 259–267 (2018).
46. M. Falcone *et al*., The role of bridging ligands in dinitrogen reduction and functionalization by uranium multimetallic complexes. *Nat. Chem.* **11**, 154–160 (2019).
47. J. Twilton, P. Zhang, M. H. Shaw, R. W. Evans, D. W. MacMillan, The merger of transition metal and photocatalysis. *Nat. Rev. Chem.* **1**, 0052 (2017).